

Modeling of multilevel cell memory with the BaTiO₃/Fe nanostructured multiferroic composite material

Paul André Paglan^{1,2} and Jean Pierre Nguenang^{1,3}

¹*Pure Physics Laboratory, Group of Nonlinear Physics and Complex Systems, Department of Physics, Faculty of Science, University of Douala, P.O. Box 24157, Douala, Cameroon*

²*National Committee for Development of Technologies (NCDT), Ministry of Scientific Research and Innovation, P.O. Box 1457, Yaounde, Cameroon*

³*The Abdus Salam ICTP, Strada Costiera 11, I-34151 Trieste, Italy*



(Received 25 December 2018; revised manuscript received 28 April 2019; published 16 July 2019)

In order to enhance the performance of calculators, multilevel cell (MLC) memories have been proposed as an alternative solution to improve the communication speed between their processors and memories, and also in order to increase the effective storage density of memory devices. In this Rapid Communication, we propose a model of MLC memory based on a multiferroic (MF) composite material. We introduce a one-dimensional trilayer ferromagnetic/ferroelectric/ferromagnetic MF composite material through which we investigate theoretically the dynamics of an electromagnon excitation displaying a soliton structure with an envelope shape. It emerges from this study based on barium titanate (BaTiO₃) and iron (Fe) that, for suitable values of the parameters of a single initial polarization excitation, some propagation scenarios display the encoding of the states of a system of two magnetic bits, i.e., the **11**, **10**, **01**, and **00** states. In addition to this result, it is also realized that the system exhibits another scenario for which the signal propagating in the MF material is alternately converted from an electrical signal into a magnetic signal and reversely. Such outcomes suggest, on the one hand, the possibility to model a four-level MLC memory, and on the other hand, the modeling of an electromagnetic oscillator, based on a MF composite material.

DOI: [10.1103/PhysRevB.100.020404](https://doi.org/10.1103/PhysRevB.100.020404)

Introduction. Computer memories could be seen as arrays of memory cells in which we can store bits of data. For conventional memories, the memory cells, so-called single-level cell (SLC) memory, allow one to store only one bit of data per cell, i.e., it allows one to encode the states **0** and **1**. However, the increasing interest in obtaining better performing calculators, i.e., higher-density chips and faster communication between the processor and the memory, have led to the development of a new class of memories that include multilevel cell (MLC) memories, in which we can store multiple bits of data in one cell [1,2]. For instance, with a four-level cell memory, we can store two bits of data in one memory cell, i.e., we can encode the states **11**, **10**, **01**, and **00**. Nowadays, the MLC technique appears as one of the prevalent techniques to achieve an extremely low bit cost in random access memory (RAM) such as resistive RAM (RRAM), phase-change RAM (PCRAM), spin-transfer-torque magnetoresistive RAM (STT-MRAM), and Flash memory [3,4]. In this Rapid Communication, our study is focused on exploring the possibility of modeling a MLC memory based on multiferroic (MF) materials, which are well acknowledged to exhibit unusual physical properties. Indeed, MF materials are peculiar materials that possess at least two ferroic orders, among which are the ferroelectric (FE) order, the ferromagnetic (FM) order, the ferroelastic order, and the ferrotoroidic order [5]. In the particular case for which the ferroelectric and the ferromagnetic orders coexist in such materials, the magnetoelectric coupling between these two orders allows one to control magnetization (polarization) by means of an

electric field (magnetic field) [6–11], which may be used for new device applications [12–15]. So, from the application point of view of MF composite materials, the energy from the FE part may induce the magnetization reversal process in the FM part. Such a process opens the way to the control of the magnetization dynamics with an electrical excitation which is less expensive in energy than that of an equivalent magnetic excitation, which is one of the central issues of modern magnetic device technologies. Hence potential applications include quantum computers, devices for memory, magnetic sensors, and so on. Several studies have been done on the bilayer BaTiO₃/Fe MF composite material, which allowed one to well understand the magnetoelectric effect in this structure [8,16–18], and to reveal new features based on the dynamics of electromagnon excitations [19–21]. With the aim to provide, from the application point of view, other features of this MF composite material through the dynamics of electromagnon excitations, we introduce a trilayer MF composite material. This model is composed of two FM components of iron (Fe) separated by one FE component of barium titanate (BaTiO₃) (see Fig. 1). The outline of this Rapid Communication is as follows. In Sec. II, the dynamics of electromagnon excitations through the trilayer MF composite material is modeled by means of the Landau-Khalatnikov-Tani (LKHT) and the Landau-Lifshitz-Gilbert (LLG) equations, in a model of a one-dimensional chain. In Sec. III, we present the results obtained by numerical simulations of the equations generated in Sec. II, and we discuss them, namely, a model of a four-level MLC memory and a model

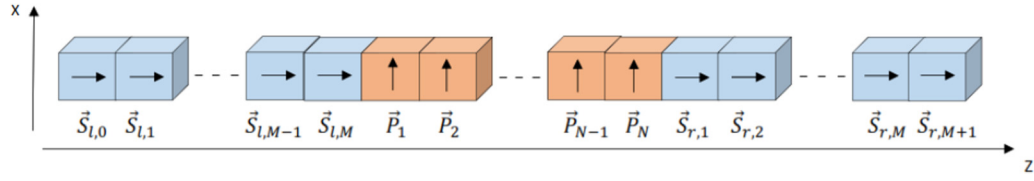


FIG. 1. A trilayer ferroelectric (orange) and ferromagnetic (blue) multiferroic composite material. As in the previous studies on the bilayer model, the trilayer MF material is discretized in a coarse-grained approach. All cells are cubic cells of equal volume a^3 , with $a = 1[\text{nm}]$; the polarization \vec{P}_n is a one-component vector along the x axis, i.e., $\vec{P}_n = (P_n, 0, 0)$, whereas the magnetization described by the spins $\vec{S}_{l,i}$ and the spins $\vec{S}_{r,j}$ are vectors that display three components, i.e., $\vec{S}_{l,i} = (S_{l,i}^x, S_{l,i}^y, S_{l,i}^z)$ and $\vec{S}_{r,j} = (S_{r,j}^x, S_{r,j}^y, S_{r,j}^z)$. We also consider that the polarization and the magnetization are orthogonal in the equilibrium configuration [19,20]: $\vec{P}_n = (P, 0, 0)$, $\vec{S}_{l,i} = (0, 0, S)$, and $\vec{S}_{r,j} = (0, 0, S)$. The indices l and r refer to the left and right FM components, whereas n and i or j correspond to the site positions of the polarization and the spins in the MF material, respectively.

of an electromagnetic oscillator. Section IV contains some concluding remarks.

Theoretical formulation. We describe the dynamics of the electromagnon excitations through the MF composite material by means of the LKdT [22,23] and the LLG equations [16,17], for the polarization and the magnetization, respectively. Using the free energy of the system (see the Appendix), these equations lead to the following dimensionless equations,

$$\frac{d^2 p_n}{dt^2} = -\alpha p_n - \beta p_n^3 + \zeta(p_{n+1} - 2p_n + p_{n-1}) + \lambda_p s_{l,M}^x \delta_{n,1} + \lambda_p s_{r,1}^x \delta_{n,N}, \quad (1)$$

$$\frac{ds_{l,i}^x}{dt} = J[s_{l,i}^z (s_{l,i-1}^y + s_{l,i+1}^y) - s_{l,i}^y (s_{l,i-1}^z + s_{l,i+1}^z)] - 2K s_{l,i}^y s_{l,i}^z, \quad (2)$$

$$\frac{ds_{l,i}^y}{dt} = J[s_{l,i}^x (s_{l,i-1}^z + s_{l,i+1}^z) - s_{l,i}^z (s_{l,i-1}^x + s_{l,i+1}^x)] + 2K s_{l,i}^x s_{l,i}^z - \lambda_s p_1 s_{l,M}^z \delta_{i,M}, \quad (3)$$

$$\frac{ds_{l,i}^z}{dt} = J[s_{l,i}^y (s_{l,i-1}^x + s_{l,i+1}^x) - s_{l,i}^x (s_{l,i-1}^y + s_{l,i+1}^y)] + \lambda_s p_1 s_{l,M}^y \delta_{i,M}, \quad (4)$$

$$\frac{ds_{r,j}^x}{dt} = J[s_{r,j}^z (s_{r,j-1}^y + s_{r,j+1}^y) - s_{r,j}^y (s_{r,j-1}^z + s_{r,j+1}^z)] - 2K s_{r,j}^y s_{r,j}^z, \quad (5)$$

$$\frac{ds_{r,j}^y}{dt} = J[s_{r,j}^x (s_{r,j-1}^z + s_{r,j+1}^z) - s_{r,j}^z (s_{r,j-1}^x + s_{r,j+1}^x)] + 2K s_{r,j}^x s_{r,j}^z - \lambda_s p_N s_{r,1}^z \delta_{j,1}, \quad (6)$$

$$\frac{ds_{r,j}^z}{dt} = J[s_{r,j}^y (s_{r,j-1}^x + s_{r,j+1}^x) - s_{r,j}^x (s_{r,j-1}^y + s_{r,j+1}^y)] + \lambda_s p_N s_{r,1}^y \delta_{j,1}. \quad (7)$$

The dimensionless parameters that appear in these equations are related to the real parameters as follows: $\vec{p}_n = \vec{P}_n/P$, $\vec{s}_{l,i} = \vec{S}_{l,i}/S$, $\vec{s}_{r,j} = \vec{S}_{r,j}/S$, $t = \omega_0 t[\text{s}]$, $\alpha = \frac{1}{\mu\omega_0^2} \tilde{\alpha}$, $\beta = \frac{P^2}{\mu\omega_0^2} \tilde{\beta}$, $\zeta = \frac{1}{\mu\omega_0^2} \tilde{\zeta}$, $K = \frac{\gamma S}{\omega_0} \tilde{K}$, $J = \frac{\gamma S}{\omega_0} \tilde{J}$, $\lambda_p = \frac{S}{\mu\omega_0^2 P} \tilde{\lambda}$, $\lambda_s = \frac{\gamma P}{\omega_0} \tilde{\lambda}$. Here, the parameters P , S , μ , and γ are the values of polarization and spins at the equilibrium configuration, a kinetic coefficient,

and the gyromagnetic ratio, respectively. The parameters $\tilde{\alpha}$ and $\tilde{\beta}$ correspond to the coefficients of the Ginzburg-Landau-Devonshire (GLD) potential and the $\tilde{\zeta}$ parameter is the coefficient of the linear intersite coupling energy for the polarization, whereas $\omega_0 = \sqrt{\frac{\tilde{\zeta}}{\mu}}$ is a characteristic frequency. The parameters \tilde{K} , \tilde{J} , and $\tilde{\lambda}$ are set for the coefficients of the anisotropy energy, the exchange energy, and the magnetoelectric coupling energy, respectively.

Numerical results and discussion For the numerical simulations, we used an envelope soliton excitation as the initial condition of the polarization, i.e., $p_n = A \cos[q(n - n_0)] \text{sech}[(n - n_0)/L]$, with A , L , and q the amplitude, the width, and the wave number, respectively. The parameter n_0 is the initial position of the excitation in the FE part of the MF material. Then we chose the values of the dimensionless parameters of the MF material as follows: $\alpha = 0.2$, $\beta = 0.1$, $\zeta = 1$, $K = 0.6$, $J = 1$, and $\lambda_p = \lambda_s = 1$ [19,21]. The estimated values in SI units of the related real parameters are given in the Appendix. Finally, we used fixed boundary conditions, i.e., $s_{l,0}(t) = 0$ and $s_{r,M+1}(t) = 0$, to the edges of the MF material. The energy density plotted corresponds to the local dimensionless values of the MF Hamiltonian $H = F + \sum_{n=1}^N [\frac{\mu}{2} \dot{\vec{P}}_n]^2 a^3$, with F corresponding to the free energy of the MF composite material (see the Appendix) and the sum on n representing the kinetic energy of the FE part [19,20]. The time displayed on the figures is in dimensionless units (d.u.), and the time in SI units (in seconds) is obtained via the relation $t[\text{d.u.}] = \omega_0 t[\text{s}]$. In Refs. [19,20,24], ω_0 is given by $\omega_0 \sim 10^{12} \text{ s}^{-1}$, therefore $t[\text{s}] \sim 10^{-12} t[\text{d.u.}]$. Thus, the timescale on the figures displayed is of the order of $\sim 10^{-9} \text{ s}$.

a. Multilevel cell memory Let us remind that, generally speaking in classical information, a bit is the elementary information unit. It can be realized by a system that can remain only in two states, which are encoded traditionally by **0** and **1**. For instance, a bit may correspond to a capacitor (charged/discharged), an interceptor (on/off), the magnetization or the polarization of one domain (up/down), and so on. Thus, the left and the right FM components of our MF material could appear as a system of two magnetic bits for which the state **1** or **0** of each bit corresponds to the presence or the absence of a solitary wave, respectively. From this point of view, some results obtained in our study show the possibility to control electrically the states of both bits with

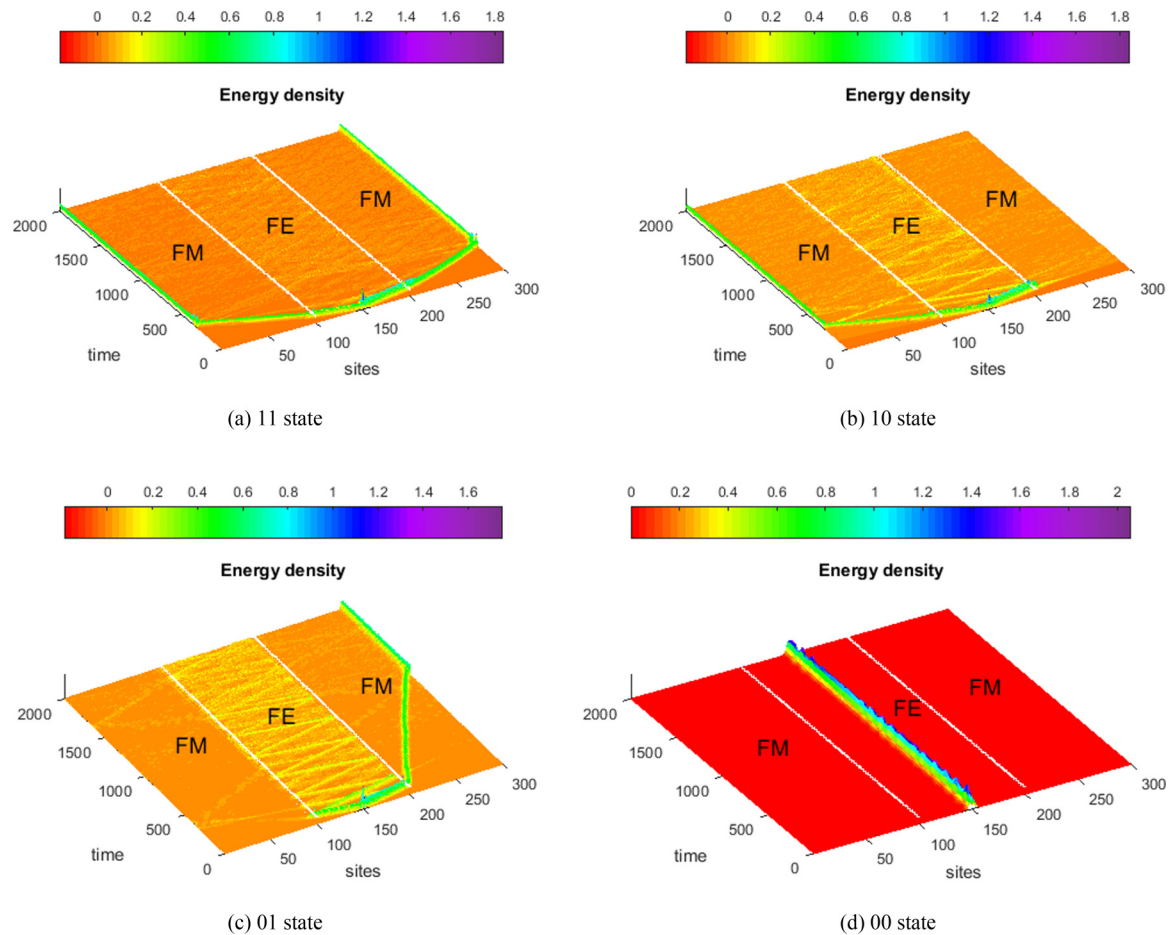


FIG. 2. Modeling of a four-level MLC memory with a trilayers FM/FE/FM MF composite material: Simultaneous control of two magnetic bits by means of an electrical excitation. The electrical excitation, i.e., the excitation of the polarization, is done at the middle of the FE part of the MF material. The two bit states on(a)–(d) correspond to the wave number values $q = 1, q = 1.2, q = 0.85,$ and $q = 3.1,$ respectively. We set $A = 2$ and $L = 10/3.$

a single excitation. Indeed, as we can see in Fig. 2, suitable values of the parameters of the initial polarization excitation allow one to get some propagating scenarios which allow one to encode the states **11**, **10**, **01**, and **00**, as follows: One pinned solitary wave in both the left and the right FM parts of the MF components [i.e., the **11** state, see Fig. 2(a)], one pinned solitary wave in the left part and no solitary wave in the right part [i.e., the **10** state, see Fig. 2(b)], no solitary wave in the left part and one pinned solitary wave in the right part [i.e., the **01** state, see Fig. 2(c)], and finally no solitary wave in both the left and the right FM parts of the MF material [i.e., the **00** state, see Fig. 2(d)]. These propagating scenarios could be explained as follows. Owing to the fact that a planar wave can be modulated spontaneously in a nonlinear medium [25], the initial excitation in our system can also undergo a spontaneous modulation due to the harmonics that emerges because of the nonlinearity of the medium. This modulation can continue until the initial excitation is split into wave packets. There are two wave packets in our case, each spreading with its own frequency. Indeed, the amplitude modulation of a wave can lead to two waves whose frequencies, usually called lateral frequencies, are symmetrical in relation to the frequency ω of the initial signal: $\omega - \delta\omega$ and $\omega + \delta\omega$ [26]. For our system, $\delta\omega$ stands as the frequency offset due to the effects of the

nonlinear property of the medium [19]. From the foregoing, owing to the nonlinear nature of the system, when one of the components of the initial excitation acquires a frequency that belongs to the FM frequency band, it is transmitted in the FM part of the MF material, since it is resonant with the FM excitation modes. If not, it is reflected at the FE/FM interface. As a result, for the **11** state, the frequencies of both components of the initial excitation belong to the FM frequency band. For the case of the **10** state, only the frequency of the left component belongs to the FM band, while for the **01** state, only the frequency of the right component belongs to the FM frequency band. However, the **00** state is obtained when the initial excitation does not possess enough kinetic energy to escape from the GLD potential. It is then trapped and the system displays a stationary solitary wave. In Fig. 3, we display explicitly these four states at the times before and after the pinning of the solitary wave at the FM edges. Based on these results, our trilayer MF composite material appears as a MLC memory (four-level cell memory) in which we can store two bits of data. Unlike the case of memories based on SLC, those with MLC offer singularly the advantages to get higher-density storage and lower cost per bit. These types of memories enable also a faster communication between the processor and the memory. This is based on the fact

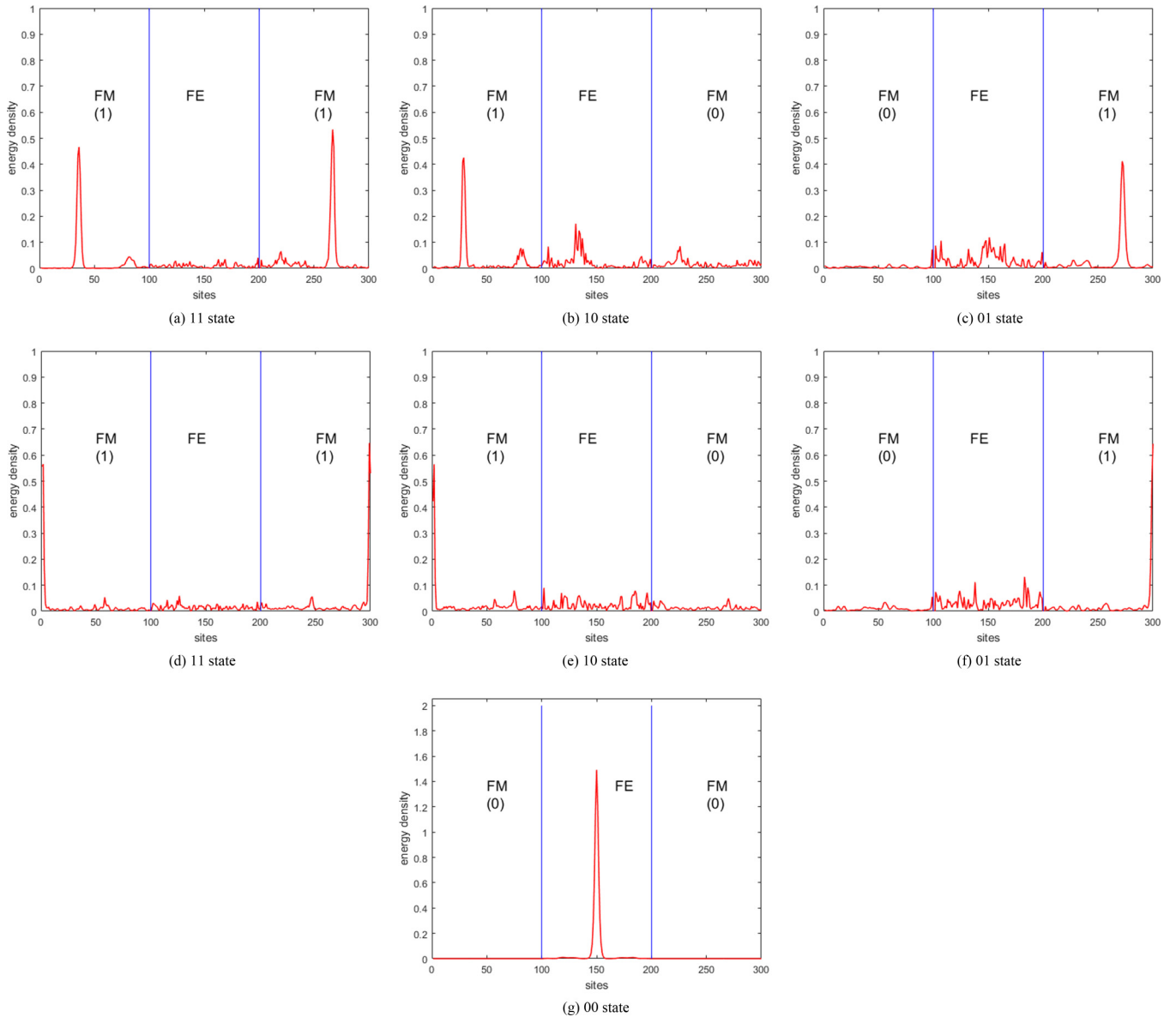


FIG. 3. The **11**, **10**, and **01** two-bit state profiles at a time (a)–(c) before and (d)–(f) after the pinning of the solitary wave at the FM edges, and the **00** two-bit state profile at (g).

that the number of memory cells enabling access for writing and reading data is reduced. However, such memories also display disadvantages on energy consumption and lack of sustainability. Meanwhile, the model of MLC memory that we propose could serve to solve these two inconveniences. For instance, the fact that we use an electrical excitation to write the data and not a magnetic excitation allows us to achieve a considerable energy gain. It could display also a better sustainability because it is composed of two components, each of which supports only two states as a single bit, and not as in some previous models that are composed only with one component supporting all the states of the MLC memory.

b. Electromagnetic oscillator Besides the results shown in Figs. 2 and 3, the outcome displayed in Figs. 4(a) or 4(b) shows a system in which the information appears and disappears alternatively in the FM components and the FE component of the MF material. Indeed, contrary to the pre-

vious cases, the solitary wave is not pinned at the edges of the MF material. It is reflected at the edges, allowing then its propagation along the material from one edge to another. Thus, during the propagation of the solitary wave in the MF material, considering its conversion into a magnetic signal, i.e., the presence of the solitary wave in the left or in the right FM component, as state **1** of the MF material, and its conversion into an electrical signal, i.e., the presence of the solitary wave in the FE component, as state **0**, the MF material appears as an oscillator, whose states alternate in the time between one electrical state and one magnetic state, as seen in Fig. 4(c). Let us notice that these oscillations are produced by a single excitation of the polarization, and they can last for a while. However, if we need to maintain the electromagnetic oscillations of the system, we can reexcite the polarization to refresh them every time that the oscillations tend to vanish. From an application point of view, such an electromagnetic

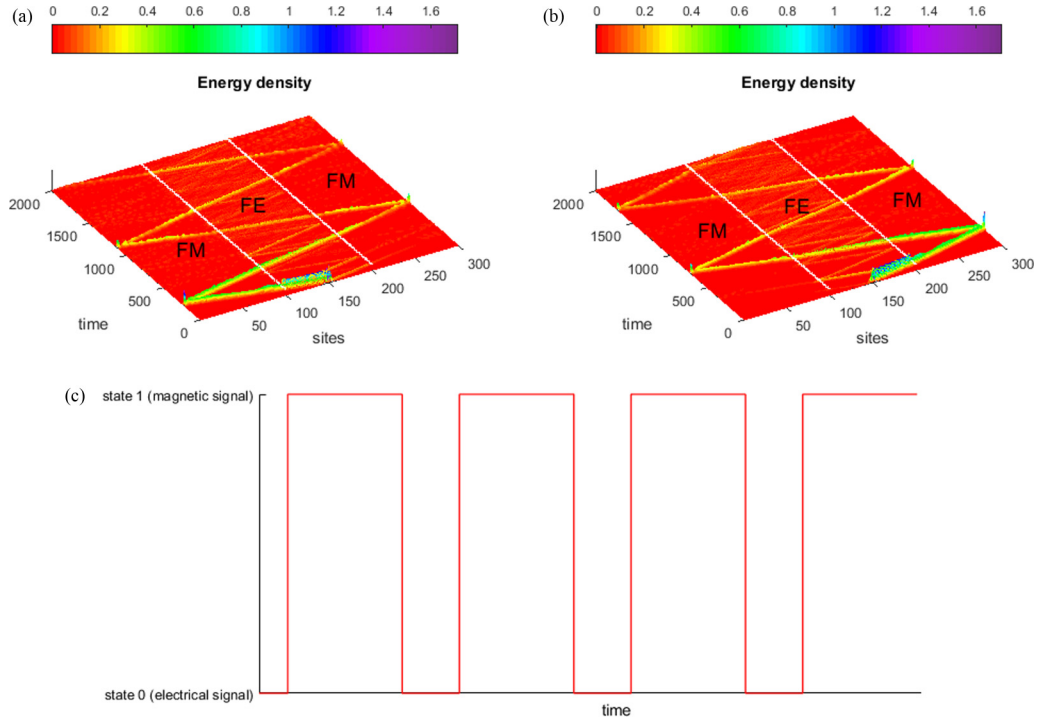


FIG. 4. Modeling of an electromagnetic oscillator with a trilayer FM/FE/FM MF composite material. (a) or (b) display an electromagnetic oscillator in which the information is transformed alternately into an electrical signal and into a magnetic signal, during its propagation through the MF material. The excitation of the polarization that is responsible for these oscillations is done in the middle of the FE component. Its amplitude and its width are fixed to $A = 0.7$ and $L = 10/3$. For (a) the wave number is fixed to $q = 5$ and for (b) it is fixed to $q = 7.5$. (c) displays the evolution in a logic representation of the states of the electromagnetic oscillator displayed in (a) or (b). The magnetic alternations of the signal last twice as long as the electric alternations.

oscillator can be used as a converter of electrical signals into magnetic signals, and reciprocally. It can also be used simply as an oscillator to generate a clock signal for applications in logic circuits.

Conclusion. Through a one-dimensional trilayer MF composite material (FM/FE/FM) based on barium titanate (BaTiO_3) and iron (Fe), we studied the dynamics of an electromagnon excitation which has an envelope shape of a soliton excitation. For suitable values of the parameters of the initial polarization excitation, we showed theoretically by numerical simulation that with a single polarization excitation, it is possible, on the one hand, to encode simultaneously the states of a system of two bits, which correspond to the right and left FM components of the MF material, i.e., to model a four-level MLC memory, and, on the other hand, to model an electromagnetic oscillator. The outcome of this investigation is interesting enough to realize powerful devices for calculations and memory operations, with MF materials. However, from the results obtained here, many other investigations, both theoretical and experimental, need to be engaged in order to synthesize MLC memories based on this model. For instance, we suggest the study of the effect of long-range dipolar interactions and the effect of nonlinear magnetoelectric coupling for higher-energy excitations. Other studies based on other models with the use of asymmetric FM electrodes such as iron and cobalt, and the use of lead zirconate titanate (PZT) as an alternative to BaTiO_3 needs to be engaged. All these issues will be considered in our subsequent investigations.

Acknowledgments. J.P.N. acknowledges helpful discussions with Prof. S. Ruffo in some aspects of this work, as well as the support of the Condensed Matter Group at ICTP, and the warm hospitality of the Statistical Physics Group at SISSA in Trieste.

Appendix. To describe the dynamics of electromagnon excitations in the MF composite material, we use the following Landau-Khalatnikov-Tani (LKht) and Landau-Lifshitz-Gilbert (LLG) equations,

$$\mu \frac{d^2 \vec{P}_n}{dt^2} = \vec{E}_n = -\frac{1}{a^3} \frac{\partial F}{\partial \vec{P}_n}, \quad (\text{A1})$$

$$\frac{d\vec{S}_{l,i}}{dt} = -\gamma \vec{S}_{l,i} \wedge \vec{H}_{l,i} = -\gamma \vec{S}_{l,i} \wedge \left(-\frac{1}{a^3} \frac{\partial F}{\partial \vec{S}_{l,i}} \right), \quad (\text{A2})$$

$$\frac{d\vec{S}_{r,j}}{dt} = -\gamma \vec{S}_{r,j} \wedge \vec{H}_{r,j} = -\gamma \vec{S}_{r,j} \wedge \left(-\frac{1}{a^3} \frac{\partial F}{\partial \vec{S}_{r,j}} \right). \quad (\text{A3})$$

In these equations, we neglected the damping terms, considering as in Ref. [20] that the dissipation has no qualitative effects for the so considered length and the timescale signal transmission ($\sim 10^{-9}$ s). The parameters \vec{E}_n , $\vec{H}_{l,i}$, $\vec{H}_{r,j}$, μ , and γ appearing in these equations correspond to the effective electric field acting on the on-site polarization \vec{P}_n , the effective magnetic fields acting on the on-site magnetization $\vec{S}_{l,i}$ and $\vec{S}_{r,j}$, a kinetic coefficient, and the gyromagnetic ratio, respectively. F is the free energy of the trilayer MF composite material, and it corresponds to the sum of the FE, FM, and the

TABLE I. Estimated values of the parameters of the iron and barium titanate components of the multiferroic material [19,20,24].

Parameters	Values	Units
$\tilde{\alpha}$	2.77×10^7	V m/C
$\tilde{\beta}$	1.7×10^8	V m ⁵ /C ³
$\tilde{\zeta}$	1.3×10^8	[V m/C]
$\tilde{J}a^3$	3.15×10^{-20}	J
$\tilde{K}a^3$	6.75×10^{-21}	J
γ	1.76×10^{11}	(Ts) ⁻¹
$\tilde{\lambda}$	Parameter	V m ²
a	1×10^{-9}	m
ω_0	$\sim 10^{12}$	s ⁻¹
P	0.265	C/m ²
$M = \gamma S$	1.71×10^6	A/m

magnetolectric free energies [16,19],

$$F = F_P + F_{S_l} + F_{S_r} + F_{PS}. \quad (\text{A4})$$

The FE free energy is given by

$$F_P = \sum_{i=1}^N \left[\frac{\tilde{\alpha}}{2} \tilde{P}_i^2 + \frac{\tilde{\beta}}{4} \tilde{P}_i^4 + \frac{\tilde{\zeta}}{2} (\tilde{P}_{i+1} - \tilde{P}_i)^2 \right] a^3. \quad (\text{A5})$$

The terms with $\tilde{\alpha}$ and $\tilde{\beta}$ parameters correspond to the Ginzburg-Landau-Devonshire (GLD) potential and the terms with the $\tilde{\zeta}$ parameter are the linear intersite coupling energies.

For the left and the right FM parts, the free energies are

$$F_{S_l} = \sum_{i=1}^M [-\tilde{K}(\tilde{S}_{l,i}\tilde{u}_z)^2 - \tilde{J}\tilde{S}_{l,i}\tilde{S}_{l,i+1}]a^3, \quad (\text{A6})$$

$$F_{S_r} = \sum_{j=1}^M [-\tilde{K}(\tilde{S}_{r,j}\tilde{u}_z)^2 - \tilde{J}\tilde{S}_{r,j}\tilde{S}_{r,j+1}]a^3. \quad (\text{A7})$$

The terms with the parameter \tilde{K} are set for the anisotropy energy while the others with the \tilde{J} parameter correspond to the exchange energy.

The magnetolectric coupling energy corresponds to

$$F_{PS} = (-\tilde{\lambda}\tilde{P}_l\tilde{S}_{l,M})a^3 + (-\tilde{\lambda}\tilde{P}_N\tilde{S}_{r,1})a^3, \quad (\text{A8})$$

where the parameter $\tilde{\lambda}$ represents the magnetolectric coupling coefficient. In Table I we give the estimated values of the parameters appearing in the free energy of the system, and the values of polarization and magnetization in the equilibrium configuration.

- [1] S. C. Park, J. J. Kong, Y. H. Lee, and D. K. Kang, Multi-level cell memory device and method thereof, U.S. Patent No. 7,962,831 B2 (14 June 2011).
- [2] N. Muralimanohar, H. B. Yoon, and N. P. Jouppi, Multi-level cell memory, U.S. Patent No. 9,443,580 B2 (13 September 2016).
- [3] M. Bauer, R. Alexis, G. Atwood, B. Baltar, A. Fazio, K. Frary, M. Hensel, M. Ishac, J. Javanifard, M. Landgraf *et al.*, in *Proceedings ISSCC '95 - International Solid-State Circuits Conference* (IEEE, New York, 1995), pp. 132–133.
- [4] J.-C. Liu, C.-W. Hsu, I.-T. Wang and T.-H. Hou, *IEEE Trans. Electron Devices* **62**, 2510 (2015).
- [5] K. Dörr, *Magnetolectric Multiferroics*, presented at the European School on Magnetism, 2007, <http://magnetism.eu/esm/2007-cluj/abs/Doerr1-abs.pdf> (unpublished).
- [6] M. Fiebig, *J. Phys. D* **38**, R123 (2005).
- [7] W. Eerenstein, N. D. Mathur, and J. F. Scott, *Nature (London)* **442**, 759 (2006).
- [8] C.-G. Duan, S. S. Jaswal, and E. Y. Tsymlal, *Phys. Rev. Lett.* **97**, 047201 (2006).
- [9] G. Lawes and G. Srinivasan, *J. Phys. D: Appl. Phys.* **44**, 243001 (2011).
- [10] C.-L. Jia, T.-L. Wei, C.-J. Jiang, D.-S. Xue, A. Sukhov, and J. Berakdar, *Phys. Rev. B* **90**, 054423 (2014).
- [11] Y. Wang, Y. Su, J. Li, and G. J. Weng, *J. Appl. Phys.* **117**, 164106 (2015).
- [12] N. Spaldin and M. Fiebig, *Science* **309**, 391 (2005).
- [13] R. Ramesh and N. A. Spaldin, *Nat. Mater.* **6**, 21 (2007).
- [14] M. Ghidini, R. Pellicelli, J. L. Prieto, X. Moya, J. Soussi, J. Briscoe, S. Dunn, and N. D. Mathur, *Nat. Commun.* **4**, 1453 (2013).
- [15] M. Ghidini, F. Maccherozzi, X. Moya, L. C. Phillips, W. Yan, J. Soussi, N. Métallier, M. E. Vickers, N.-J. Steinke, R. Mansell *et al.*, *Adv. Mater.* **27**, 1460 (2015).
- [16] A. Sukhov, C. Jia, P. P. Horley, and J. Berakdar, *J. Phys.: Condens. Matter* **22**, 352201 (2010).
- [17] P. P. Horley, A. Sukhov, C. Jia, E. Martinez, and J. Berakdar, *Phys. Rev. B* **85**, 054401 (2012).
- [18] C. Jia, A. Sukhov, P. P. Horley, and J. Berakdar, *Europhys. Lett.* **99**, 17004 (2012).
- [19] L. Chotorlishvili, R. Khomeriki, A. Sukhov, S. Ruffo, and J. Berakdar, *Phys. Rev. Lett.* **111**, 117202 (2013).
- [20] R. Khomeriki, L. Chotorlishvili, B. A. Malomed, and J. Berakdar, *Phys. Rev. B* **91**, 041408(R) (2015).
- [21] P. A. Paglan, J. P. Nguenang, and S. Ruffo, *Europhys. Lett.* **122**, 68001 (2018).
- [22] K. Tani, *J. Phys. Soc. Jpn.* **26**, 93 (1969).
- [23] S. Sivasubramanian, A. Widom, and Y. N. Srivastava, *Ferroelectrics* **300**, 43 (2004).
- [24] L. Chotorlishvili, S. R. Etesami, J. Berakdar, R. Khomeriki, and J. Ren, *Phys. Rev. B* **92**, 134424 (2015).
- [25] M. Peyrard and T. Dauxois, *Physique des Solitons* (EDP Sciences, Paris, 2004).
- [26] T. Neffati, *Électronique de A à Z* (Dunod, Paris, 2006).